BMC Ophthalmology

RESEARCH

Open Access

Assessment of the effects of vitreopapillary adhesion on optic disc and macular parameters, and peripapillary choroidal vasculature

Ziya Ayhan[1], Hazan Gül Kahraman[2], Pelin Kiyat[2*] and Omer Karti[1]

Abstract

Background To investigate the effects of vitreopapillary adhesion (VPA) on optic disc and macular parameters and on the peripapillary choroidal vasculature.

Methods This retrospective study included 47 eyes of 47 participants with VPA, all of whom had no history of systemic or ocular disease. Optical coherence tomography (OCT) was used to assess peripapillary retinal nerve fiber layer (RNFL) and ganglion cell complex (GCC) thickness. Images obtained from OCT were acquired and processed using ImageJ to calculate peripapillary choroidal vascular index (CVI). These measurements were then compared with those of 57 healthy controls.

Results The mean age of the study group (26 males,21 females) was 63.57 ± 6.14 years, while the mean age of the control group (29 males, 28 females) was 63.31 ± 6.86 years, with no significant differences in age ($p = 0.841$) or gender ($p = 0.652$) between the groups. All participants in the study group had stage 3 posterior vitreous detachment. Although the mean RNFL thickness was thinner in all quadrants in the study group compared to the control group, these differences were not statistically significant: inferior ($p = 0.116$), superior ($p = 0.192$), nasal ($p = 0.381$), and temporal ($p = 0.061$) quadrants. In contrast, the GCC thickness was significantly thinner in the study group than in the control group across all quadrants: inferior ($p = 0.003$), inferonasal ($p = 0.001$), inferotemporal ($p = 0.034$), superior ($p = 0.006$), superonasal ($p < 0.001$), and superotemporal ($p = 0.003$). CVI was significantly lower in the inner nasal and inner temporal regions of the study group compared to the control group ($p = 0.008$, $p < 0.001$, respectively), but no significant differences were found in the outer nasal and outer temporal regions ($p = 0.659$, $p < 0.825$, respectively).

Conclusions VMA may affect the optic disc, macular parameters, and choroidal vasculature. However, further studies with larger sample sizes are needed to confirm these findings.

Trial registration Retrospectively registered. The study followed the tenets of the Declaration of Helsinki, and it was approved by the local ethical committee (date:23.08.2023 number:2023/8-163).

Keywords Optic disc, Posterior vitreous detachment, Vitreopapillary adhesion, Vitreopapillary traction

*Correspondence:
Pelin Kiyat
pelinkiyat@hotmail.com
[1]Department of Ophthalmology, Dokuz Eylul University, İzmir, Türkiye
[2]Department of Ophthalmology, İzmir Democracy University Buca Seyfi Demirsoy Training and Research Hospital, Kozagac Mah., Ozmen Sok., No:147, Buca/iZMIR, İzmir, Türkiye

Introduction

Posterior vitreous detachment (PVD) is a common degenerative process that is characterized by the separation of the posterior vitreous cortex from the internal limiting membrane of the retina [1, 2]. The vitreous is firmly attached at the vitreous base near the ora serrata; however, its connections to the macula and optic disc are relatively weak [3]. PVD typically initiates at the perifoveal macula and progresses to the peripheral retina, with the optic disc representing the final point of attachment [4]. Abnormal PVD occurs when the vitreous undergoes liquefaction without adequate separation at the vitreoretinal interface. This can result in various complications, such as persistent adhesion and/or traction at the optic disc, known as vitreopapillary adhesion (VPA) or vitreopapillary traction (VPT), which may lead to optic nerve dysfunction [5–8]. Optical coherence tomography (OCT) enables direct visualization of the vitreopapillary interface, thereby enhancing our understanding of the underlying pathophysiology of VPT and VPA [9].

VPT is a rare and frequently disregarded condition characterized by the robust attachment of the posterior hyaloid to the optic disc and adjacent peripapillary region. VPT has its genesis in an incomplete PVD. This condition can result in the optic disc appearing elevated, which is often misidentified as optic disc edema. This can lead to the distortion of optic disc vessels and the inner retina around the peripapillary region, resulting in axonal damage. This attachment exerts a tractional force on the optic disc, leading to morphological alterations and subsequent temporary and chronic visual impairments [7–9]. Conversely, VPA is characterized by a pronounced vitreous membrane adhering to the edges of the optic disc [10]. The impact of VPA on optic disc parameters and peripapillary choroidal vascularity remains unclear. To the best of our knowledge, no existing studies have explored the impact of VPA on the optic disc, macular parameters, or peripapillary choroidal vascularity. Accordingly, the objective of this study is to examine the impact of VPA on optic disc and macular parameters, as well as on the peripapillary choroidal vascular index (CVI), utilizing Swept Source Optical Coherence Tomography (SS-OCT).

The evaluation of choroidal vascular changes in various optic nerve pathologies has been enhanced by the emergence of choroidal vascularity index (CVI), a quantitative and objective tool that can detect significant differences in choroidal vascularity between papilledema patients and healthy controls, potentially aiding in the differential diagnosis of optic disc edema. The clinical significance of CVI has been demonstrated in studies, where both total choroidal area and CVI were significantly reduced compared to healthy controls in papilledema patients, while showing no differences between active and remitted stages of papilledema, suggesting its potential role as a biomarker in optic disc pathologies [11, 12].

Methods

This retrospective study was conducted at Izmir Democracy University Buca Seyfi Demirsoy Training and Research Hospital in accordance with the approval of the local ethics committee (date:23.08.2023 number:2023/8-163). The study was conducted in accordance with the tenets set forth in the Declaration of Helsinki, and each subject provided written informed consent. The study population was retrospectively selected from patients who were examined at the ophthalmology department of İzmir Buca Seyfi Demirsoy Training and Research Hospital, Turkey. A total of 1.898 patient records between the ages of 45 and 72 years were screened for eligibility during the study period. The study included 47 eyes from 47 participants with VPA (study group) and 57 eyes from 57 healthy participants without VPA (control group).

Individuals with any systemic diseases known to affect ocular blood flow (e.g., hypertension, diabetes mellitus, renal or cardiovascular disease, migraine, anemia) were excluded from participation. Additionally, individuals with conditions that could alter ocular circulation, including pregnancy, smoking, or a history of chronic use of any topical or systemic medications (e.g., decongestants, antihistamines, sildenafil), were excluded from the study. Moreover, individuals with any condition that could compromise the accuracy of the measurements, such as refractive errors exceeding ± 3 diopters, corneal opacity, cataract, glaucoma, retinal abnormalities, nystagmus, or a history of ocular surgery or trauma, were excluded from the study. Fellow eyes used as controls in this study were specifically examined for the presence of posterior vitreous detachment (PVD) using OCT, and only eyes without PVD were included in the control group to ensure appropriate comparison with VPA study eyes.

A comprehensive ophthalmological assessment was conducted for all patients, including the determination of best-corrected visual acuity using the Snellen chart, anterior and posterior segment evaluations with slit-lamp biomicroscopy, and intraocular pressure measurement using applanation tonometry. Subsequently, SS-OCT imaging (DRI-OCT Triton, Topcon, Inc., Tokyo, Japan) was conducted on all patients to evaluate the retinal nerve fiber layer (RNFL) thickness in four quadrants (superior, temporal, inferior, and nasal) and the ganglion cell complex (GCC) thickness in six quadrants (superior, superotemporal, superonasal, inferior, inferotemporal, and inferonasal). The GCC scan protocol was used to measure the thickness of three retinal layers as a complex: RNFL, ganglion cell layer (GCL), and inner plexiform layer (IPL).

These measurements were automatically performed from the inner limiting membrane (ILM) to the outer boundary of the IPL. (Figs. 1 and 2)

Optic disc evaluation was performed using SS-OCT (DRI OCT Triton, Topcon) with an Optic Disc Cube scan protocol (12 mm × 9 mm). This scanning protocol allowed for comprehensive evaluation of the entire optic disc and surrounding area through 3D-line scanning. For RNFL and GCC measurements, we utilized the same Optic Disc Cube scan protocol, which provided detailed visualization of the entire optic disc region. Cases with nerve fiber layer traction were excluded from the study during initial screening, as the presence of traction could potentially affect the accuracy of RNFL measurements. The comprehensive nature of the 3D cube scan enabled thorough assessment of the entire optic disc area for any signs of traction.

The staging of posterior vitreous detachment (PVD) was conducted in accordance with the classification system previously established [13, 14], which divides PVD into five distinct stages. Stage 0 represents a condition in which the vitreous is entirely adhered to the retinal surface. Stage 1 is characterised by a partial separation of the vitreous from the retina, particularly in the macular area, which results in vitreomacular adhesion. In Stage 2, the vitreous has undergone partial separation from the retina, yet remains adherent to the optic disc and the nasal aspect of the disc. Stage 3 is defined by the attachment of the vitreous to the optic disc, while Stage 4 is characterised by the complete detachment of the posterior vitreous cortex from both the optic disc and the retina in the posterior pole. (Fig. 3) Two independent observers (P.K., H.G.K.) evaluated all images. In instances where there was a discrepancy between the two observers, a third expert conducted an evaluation in a blinded manner (O.K. or Z.A). In accordance with the aforementioned evaluations, patients exhibiting stage 3 PVD were selected for inclusion in the study.

The peripapillary CVI was measured in accordance with the methodology described by Kim et al. [15] The procedure for peripapillary CVI measurement is illustrated in Fig. 4. The CVI analysis was conducted using the ImageJ software (Version 1.53, National Institutes of Health, Bethesda, MD, USA). The polygon selection tool was employed to delineate the total choroidal area (TCA) between the retinal pigment epithelium and the choroid-scleral junction for the peripapillary area, within a width of 1500 µm on either side of the circular grid and within the circular grid itself. The regions of interest (ROIs) were designated in the ROI manager. Following conversion of the image to 8-bit, the Niblack autolocal thresholding tool was employed to ascertain the mean pixel value and standard deviation (SD) for all points. The luminal area (LA) was delineated using the color thresholding tool and incorporated into the ROI manager. To calculate the area of vascularity, both the LA and TCA were selected in the ROI manager and combined using an "AND" operation.

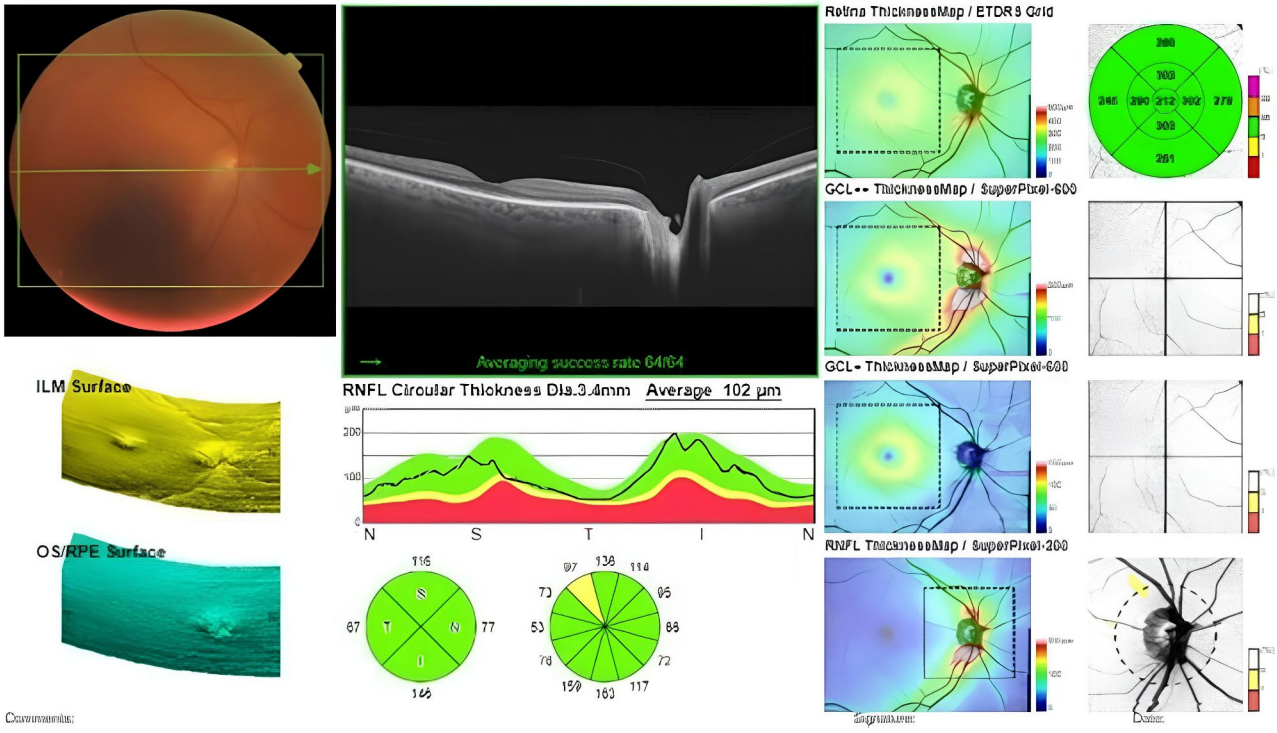

Fig. 1 Measurements of peripapillary retinal nerve fiber layer (RNFL)

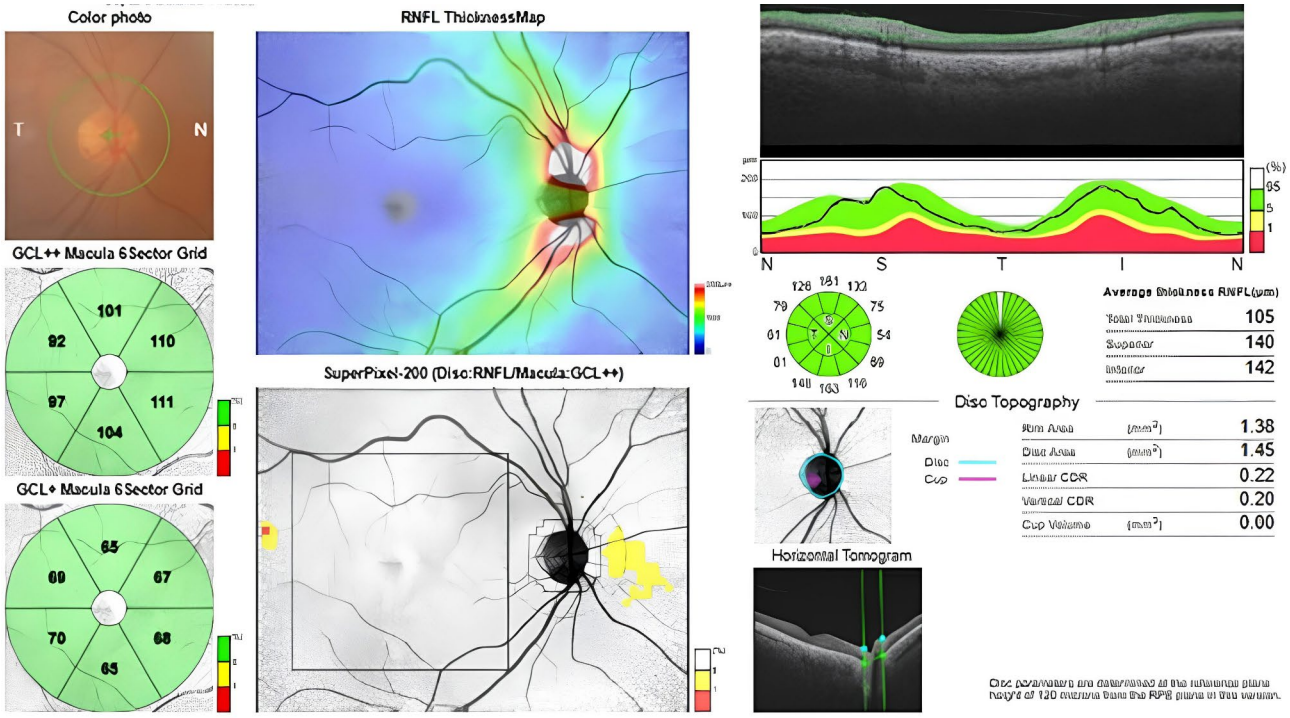

Fig. 2 Measurements of ganglion cell complex (GCC)

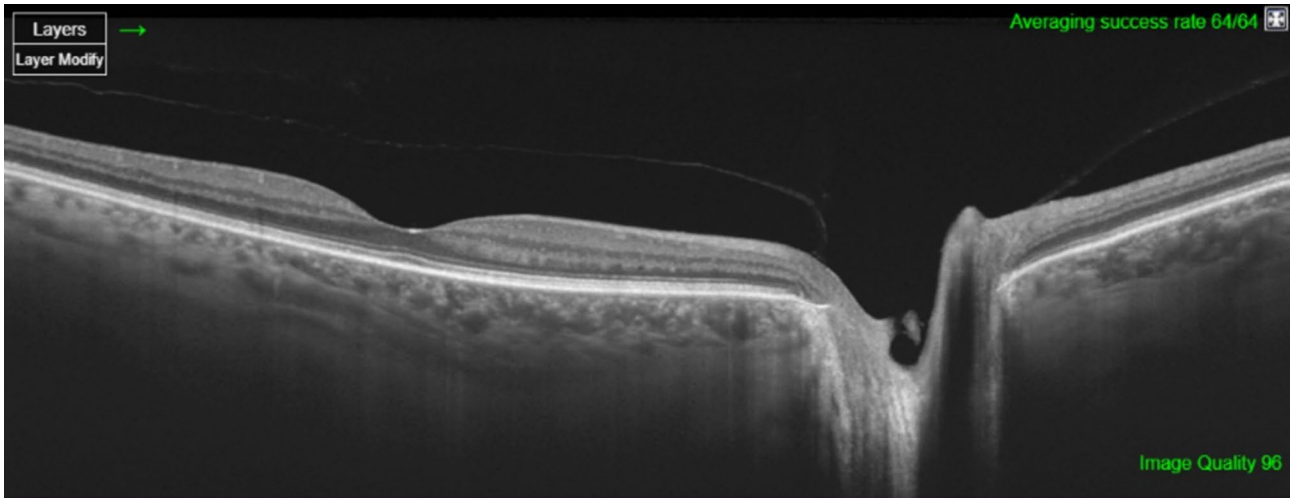

Fig. 3 Optical coherence tomography image of a stage 3 posterior vitreous detachment

Subsequently, the CVI value was calculated as the ratio of the LA to the TCA.

The data obtained from the study group were compared with those of 57 healthy volunteers who were recruited from the Buca Seyfi Demirsoy Training and Research Hospital Department of Ophthalmology for the purpose of undergoing routine examinations.

The data were analyzed using IBM SPSS Statistics, version 25. The Kolmogorov-Smirnov test was employed to ascertain the normality of the data distribution. Numerical variables were summarized as means and standard deviations or medians and ranges (minimum to maximum). The statistical analysis of differences between categorical variables was conducted using the Chi-square test. In order to compare two groups, the independent t-test was employed for data that were normally distributed, whereas the Mann-Whitney U test was utilized for data that were not normally distributed. A p-value of less than 0.05 was deemed statistically significant.

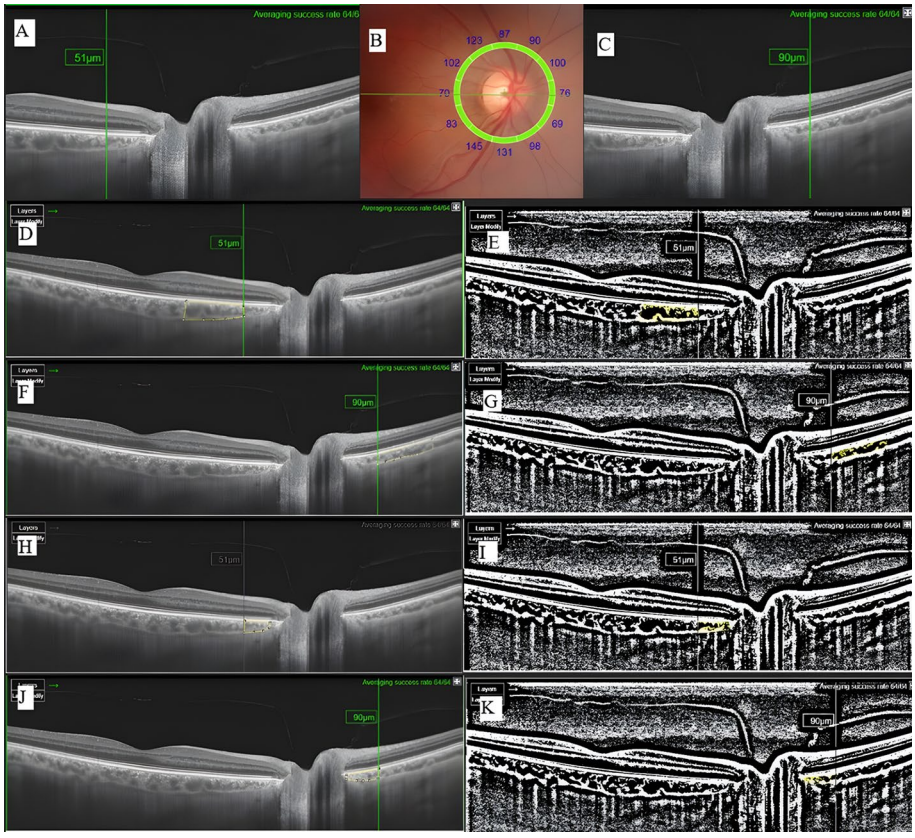

Fig. 4 Measurements of peripapillary choroidal vascular index (CVI). By clicking on the nasal rim of the retinal nerve fiber layer (RNFL) circular grid, a vertical line is placed on the B-scan image passing through the center of the RNFL circular grid. The cross point between this line and Bruch's membrane is used as the reference point (**A**, **B**, **C**). The outer nasal and outer temporal CVI measurements were obtained from regions extending 1500 microns in a temporal and nasal direction from the outer edge of the circular grid (**D**, **E**, **F**, **G**). The CVI values for the inner nasal and inner temporal regions were determined within the circular grid (**H**, **I**, **J**, **K**)

Results

The mean age of the study group ($n = 47$) was 63.57 ± 6.14 years, while the control group ($n = 57$) had a mean age of 63.31 ± 6.86 years. The study group consisted of 26 males and 21 females, while the control group included 29 males and 28 females. No statistically significant difference was observed between the two groups with regard to age ($p = 0.841$) or gender ($p = 0.652$). There was no significant difference in spherical equivalent refraction values between the patient (-1.25 ± 1.62 D) and control (-1.31 ± 1.58 D) groups ($p = 0.743$). All participants had refractive errors within ± 3 diopters to minimize the effect of refraction on OCT measurements.

A comparison of peripapillary RNFL, GCC thickness, and peripapillary CVI values between the study and control groups is presented in Table 1. Although the mean RNFL thickness was thinner in all quadrants in the study group compared to the control group, these differences were not statistically significant: inferior ($p = 0.116$), superior ($p = 0.192$), nasal ($p = 0.381$), and temporal ($p = 0.061$) quadrants. In contrast, the GCC thickness was significantly thinner in the study group than in the control group across all quadrants: inferior ($p = 0.003$), inferonasal ($p = 0.001$), inferotemporal ($p = 0.034$), superior ($p = 0.006$), superonasal ($p < 0.001$), and superotemporal ($p = 0.003$). Additionally, CVI was significantly lower in the study group compared to the control group in the inner nasal ($p = 0.008$) and inner temporal ($p < 0.001$) regions. However, no significant difference was observed between the two groups in the outer nasal ($p = 0.659$) and outer temporal ($p = 0.825$) regions.

In addition, scatter plots were created to analyze the distribution of measurements between groups (Figs. 5, 6 and 7). Figure 5 illustrates the distribution of CVI measurements, allowing for observation of choroidal vascularity patterns among participants. Figure 6 shows the distribution of RNFL thickness measurements across groups, demonstrating individual variations in RNFL thickness. The GCC thickness measurements are presented in Fig. 7, displaying the spread of GCC values between groups. These visualizations enabled detailed examination of data distribution and identification of potential outliers.

Table 1 Comparisons of RNFL, GCC and peripapillary CVI between the study group and the control group

	Study group ($n=47$)	Control group ($n=57$)	p value
RNFL thickness			
Inferior	129.74 (16.77)	134.75 (15.39)	0.116[a]
Superior	127.57 (18.84)	132.54 (19.52)	0.192[a]
Nasal	81.14 (14.68)	83.38 (11.21)	0.381[a]
Temporal	73.17 (9.24)	76.54 (8.84)	0.061[a]
GCC thickness			
Inferior	105.00 (92–130)	109.00 (90–121)	0.003[b]
Inferonasal	115.40 (9.17)	121.22 (7.62)	0.001[a]
Inferotemporal	97.36 (7.66)	100.15 (5.60)	0.034[a]
Superior	106.04 (8.32)	110.15 (6.77)	0.006[a]
Superonasal	115.87 (8.03)	121.35 (7.36)	0.000[a]
Superotemporal	93.93 (6.74)	97.73 (5.92)	0.003[a]
Peripapillary CVI			
Outer-nasal	71.43 (43–84)	71.93 (64–84)	0.659[b]
Inner-nasal	67.77 (49–79)	69.77 (61–79)	0.008[b]
Outer-temporal	70.96 (5.29)	70.77 (3.28)	0.825[a]
Inner-temporal	64.29 (40–80)	70.66 (62–84)	0.000[b]

[a] Independent t-test, [b] Mann-Whitney U test

Abbreviations: RNFL, retinal nerve fiber layer thickness; GCC, ganglion cell complex; CVI, choroidal vascular index

Discussion

The findings of this study indicate that patients with VPA demonstrated a statistically significant reduction in inner nasal and inner temporal peripapillary CVI values, as well as a significant thinning of GCC thickness. However, although a reduction in RNFL thickness was observed in all quadrants, no statistically significant differences were identified between the groups. In addition, strip plot analysis of our data demonstrated consistent distribution of values across all measurements, with no outliers or extreme values identified. This consistent distribution pattern further supports the reliability of our findings and strengthens the validity of our analyses.

The question of whether vitreopapillary interface pathologies impact the morphology and function of the optic disc, macula, and choroid remains a topic of ongoing debate in the scientific community. The current topic has been addressed in only a limited number of studies, with the majority of these focusing on VPT [16–18]. Parsa et al. [16] suggested that VPT can lead to structural changes in the optic disc. They highlighted that this process can result in various outcomes, ranging from minor, undetectable injury to complete axonal damage. The authors also noted that VPT can cause optic disc elevation, irregular dilation of the surface vessels, transient sensory phenomena, pre-papillary bleeding, and shear force injury to axons, resulting in visual field defects. In a recent study conducted by Li et al. [17], the authors investigated papillary vitreous detachment in NAION by analyzing the vitreopapillary interface between NAION patients and healthy controls. The study included 22 acute NAION patients (25 eyes), 21 non-acute NAION patients (23 eyes), and 23 healthy controls (34 eyes). Using SS-OCT, they found incomplete papillary vitreous detachment in all acute NAION patients, with higher rates of peripapillary wrinkles in acute NAION (68%) compared to non-acute NAION (30%) and controls (0%). Peripapillary superficial vessel protrusion also varied between groups (acute NAION: 44%, non-acute NAION: 91%, controls: 0%). The authors suggested that papillary vitreous detachment may contribute to NAION pathogenesis. However, in a retrospective cohort study by Thompson et al. [18], the researchers investigated eighty eyes from 74 patients with acute NAION. They found that PVD prevalence in acute NAION was only 30%, similar to unaffected contralateral eyes. Based on these findings, they concluded that VPT does not play a mechanistic role in classic NAION development, and furthermore, pre-existing PVD did not prevent NAION occurrence. While the authors found no evidence supporting VPT as a causative factor in classic NAION, they emphasized the importance of recognizing VPT optic neuropathy as a distinct clinical entity.

Beyond NAION, other studies have documented various presentations of VPT: Katz et al. [19] reported eight cases of intrapapillary and peripapillary hemorrhage associated with incomplete PVD which the affected optic discs were characterized by being small and mildly elevated, while Wisotsky et al. [6] and Nomura et al. [20] described cases of optic nerve head elevation and visual field defects caused by vitreopapillary tractional forces. In Wisotsky etl al.'s study it was suggested suggested that VPT could result in unilateral optic nerve head elevation and recommended that the posterior hyaloid be assessed in patients exhibiting optic nerve head elevation. In

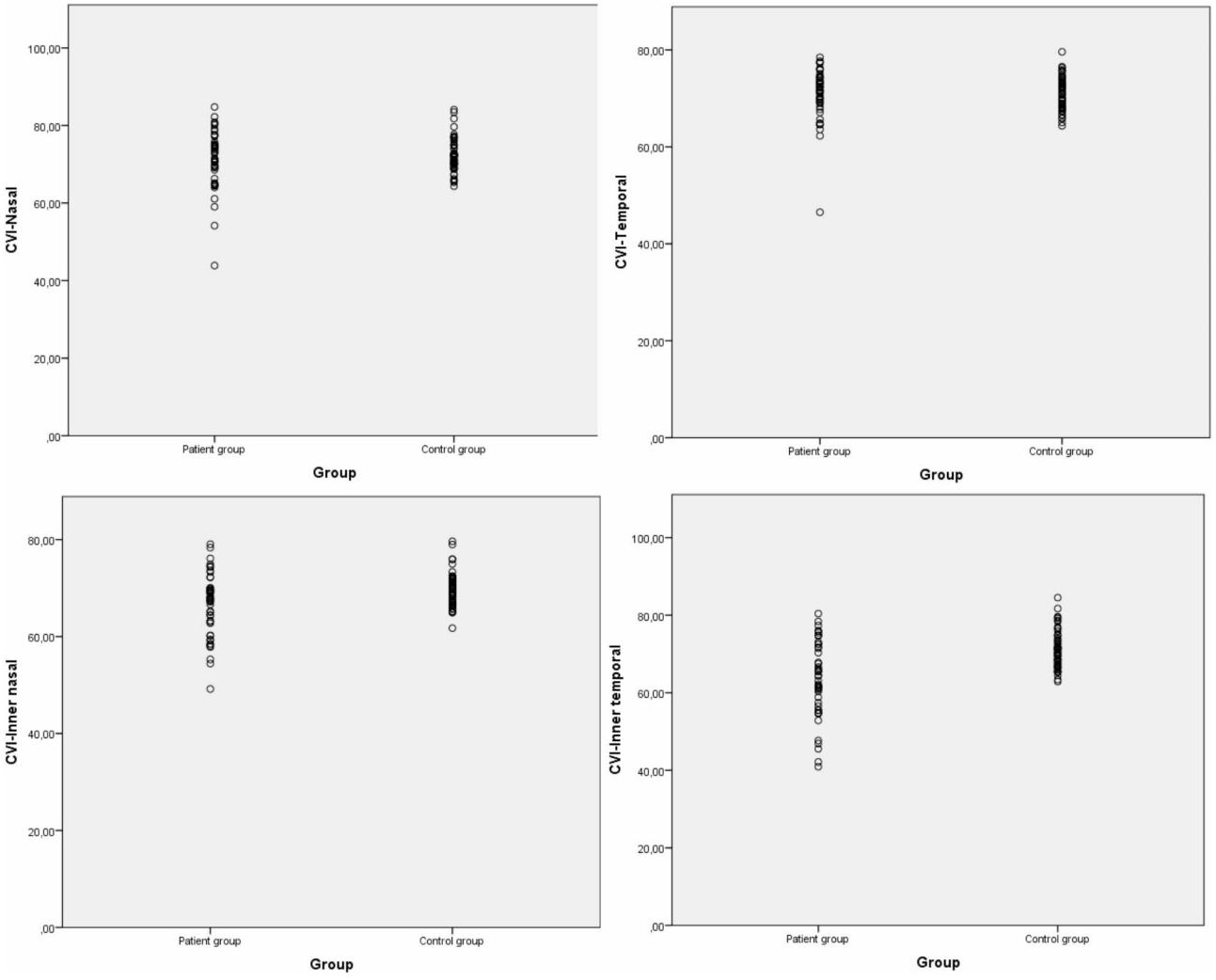

Fig. 5 Scatter plot of choroidal vascularity index (CVI) comparison between study groups

another study by Katz et al. [8], the authors reported four cases where incomplete posterior vitreous detachment and VPT led to gaze-evoked amaurosis, suggesting that vitreous traction on the optic disc can cause transient visual disturbances through nerve head elevation. Kim et al. [21] investigated the prevalence of VPT and its impact on peripapillary structure and visual function in eyes with idiopathic epiretinal membrane (ERM) and reported that more than 40% of eyes with idiopathic ERM exhibited VPT. Furthermore, VPT in these eyes was associated with changes in optic disc architecture, increased average and temporal RNFL thickness, and visual field defects. Kroll et al. [22] proposed a mechanism to explain how VPT affects visual function and impacts the optic disc. They suggested that VPT may impair the anterior optic nerve by disrupting axoplasmic flow in the optic nerve fibers and/or reducing blood flow in the posterior ciliary arteries. While the effects of these mechanisms might be reversible in the short term, they could potentially lead to irreversible optic nerve atrophy over time. Consequently, for patients with VPT, early vitrectomy should be considered as a preventive measure against optic neuropathy.

VPA is defined by the presence of a pronounced vitreous membrane adhering to the edges of the optic disc. To the best of our knowledge, no studies in the existing literature have evaluated the impact of VPA on optic disc morphology and/or function. Nevertheless, a study conducted by Sebag et al. [5] investigated the influence of VPA in macular disorders. The findings revealed that VPA was markedly more prevalent in eyes with macular holes, dry age-related macular degeneration, lamellar holes, or macular pucker compared to the control group. However, our study did not observe any of the aforementioned macular pathologies in eyes with VPA. However, the mean GCC thickness in eyes with VPA was found to be statistically significantly thinner in all quadrants when compared to the control group.

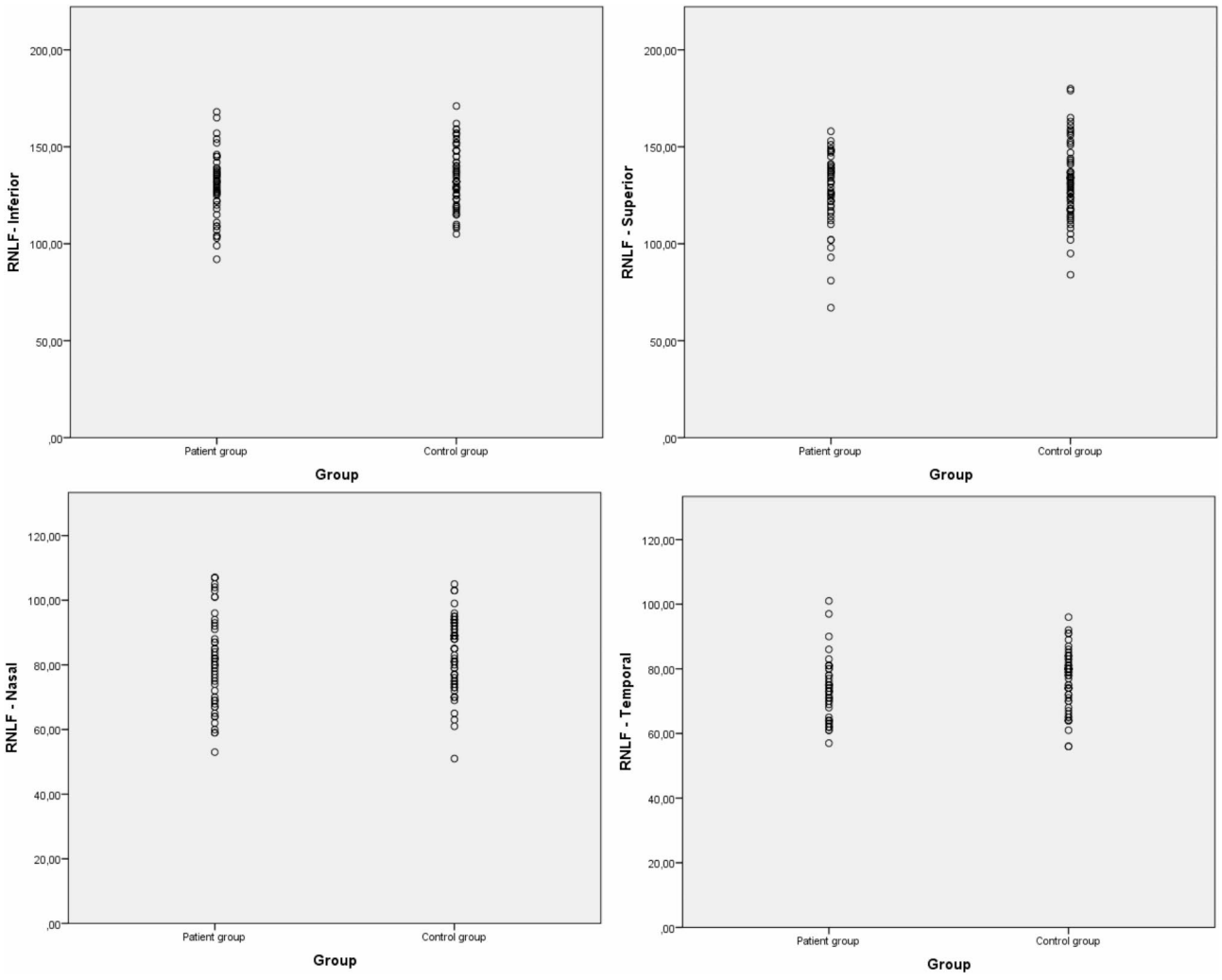

Fig. 6 Scatter plot of retinal nerve fiber layer (RNFL) thickness measurements in study groups

We consider that the persistent adhesion of the posterior hyaloid to the optic nerve head likely induced mechanical changes, resulting in the stretching of the ganglion cell axons, peripapillary retina, and superficial vessels. Such stretching can result in a reduction of both axoplasmic flow and prelaminar blood flow, which may ultimately lead to the permanent damage of axons. Therefore, a combination of mechanical and ischemic injuries may be responsible for the observed thinning of the GCC and RNFL in this study. While reductions in RNFL and GCC thickness were observed in all quadrants relative to the control group, only the GCC reduction was statistically significant. The lack of a significant difference in RNFL thickness can be attributed to two factors. Firstly, the relatively small sample size may have resulted in a lack of statistical power. A larger sample size may potentially yield statistically significant results with regard to RNFL thickness. Secondly, the absence of significant RNFL thinning in conjunction with GCC reduction may be attributed to the masking effect of VMA-related disc congestion. In contrast, a significantly lower peripapillary CVI was observed in the circular grid (inner nasal and inner temporal) in VMA patients when compared to the control group. The significance and mechanism behind this finding remain unclear, and no previous studies on this topic were identified in the literature. Given that the peripapillary choroid is responsible for nourishing the optic nerve head, we hypothesize that a reduction in CVI may increase the disc's susceptibility to ischemia. This ischemia could potentially contribute to the observed decrease in GCC and RNFL thickness, as observed in our study. However, further research is necessary to fully understand the mechanism and implications of this finding.

Although our study represents a pioneering effort in the literature, it has several notable limitations. Firstly, the sample size is relatively limited, which constrains the statistical power of the findings. Secondly, the functional

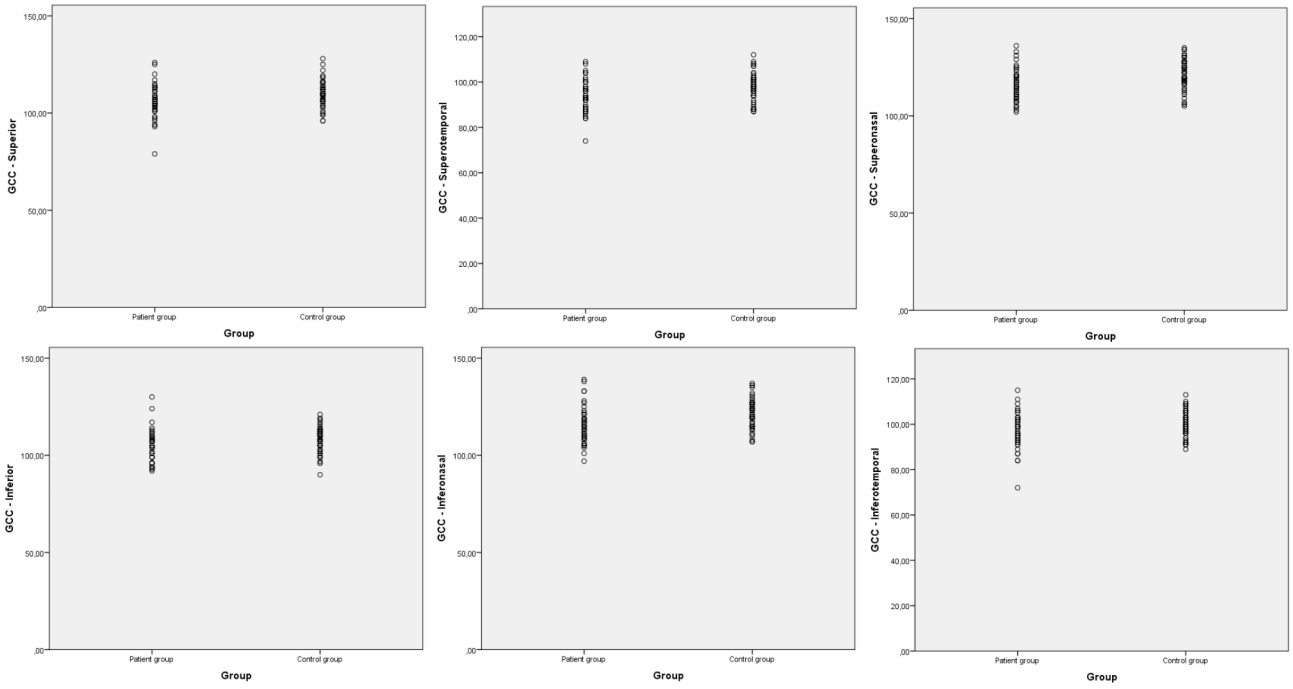

Fig. 7 Scatter plot of ganglion cell complex (GCC) thickness distribution between groups

assessment of these patients was restricted to visual acuity measurements, and the researchers were unable to conduct visual field or electrophysiological tests. Thirdly, this study is a retrospective data analysis rather than a long-term follow-up of VPA patients. Prospective data analyses would facilitate a more accurate determination of the natural course of the disease. Furthermore, the lack of axial length measurements represents a limitation, as refractive error was used to exclude eyes with high hyperopia and myopia. Moreover, we did not use the axial length correction function of Triton OCT for magnification correction in our measurements. Although there was no statistically significant difference in refractive errors between the groups, using axial length-based magnification correction could have provided more precise measurements.

Conclusions

While VPA does not exert a prominent tractional force, its adhesion may affect optic disc morphology and choroidal vascularity, potentially disrupting circulation. Further research is required to corroborate these findings, particularly through prospective studies with larger sample sizes, comprehensive functional evaluations, and OCT-angiography examinations.

Abbreviations

PVD	Posterior vitreous detachment
VPA	Vitreopapillary adhesion
VPT	Vitreopapillary traction
OCT	Optical coherence tomography
CVI	Choroidal vascular index
RNFL	Retinal nerve fiber layer
GCC	Ganglion cell complex
ERM	Epiretinal membrane

Acknowledgements

None.

Author contributions

OK, HGK, PK, ZA had full access to all of the data in the study and takes responsibility for the integrity of the data and the accuracy of the data analysis. Study concept and design: All authors. Acquisition, analysis or interpretation of data: ZA, OK, PK, HGK. Drafting of the manuscript: OK, PK, ZA, HGK. Critical revision of the manuscript for important intellectual content: All authors. Administrative, technical, or material support: PK, HGK, OK. Study supervision: OK, ZA.

Funding

None.

Data availability

The dataset used during current study are available from the corresponding author on reasonable request.

Declarations

Ethics approval and consent to participate

The study followed the tenets of the Declaration of Helsinki, and it was approved by the local ethical committee (Buca Seyfi Demirsoy Training and Research Hospital; date:23.08.2023 number:2023/8-163). Informed consent to participate was obtained from all of the participants in the study.

Consent for publication

Not Applicable.

Competing interests

The authors declare that they have no competing interests.

Received: 11 January 2025 / Accepted: 10 March 2025

Published online: 19 March 2025

References

1. Ahmed F, Tripathy K. Posterior Vitreous Detachment. In: StatPearls. Treasure Island (FL): StatPearls Publishing; 2024 Jan– 2023. PMID: 33085420.
2. Sebag J. Anomalous posterior vitreous detachment: a unifying concept in vitreo-retinal disease. Graefes Arch Clin Exp Ophthalmol. 2004;242(8):690-8. https://doi.org/10.1007/s00417-004-0980-1. PMID: 15309558.
3. Sharma S, Singh RP. Chapter 10 - Vitreoretinal Diseases, Editor(s): Arun D. Singh, Brandy C. Hayden, Ophthalmic Ultrasonography, W.B. Saunders. 2012;97–110. ISBN 9781437726367, https://doi.org/10.1016/B978-1-4377-2636-7.00010-0
4. Johnson MW. Posterior vitreous detachment: evolution and complications of its early stages. Am J Ophthalmol. 2010;149(3):371 – 82.e1. https://doi.org/10.1016/j.ajo.2009.11.022. PMID: 20172065.
5. Sebag J, Wang MY, Nguyen D, Sadun AA. Vitreopapillary adhesion in macular diseases. Trans Am Ophthalmol Soc. 2009;107:35–44. PMID: 20126480; PMCID: PMC2814571.
6. Wisotsky BJ, Magat-Gordon CB, Puklin JE. Vitreopapillary traction as a cause of elevated optic nerve head. Am J Ophthalmol. 1998;126(1):137-9. https://doi.org/10.1016/s0002-9394(98)00080-4. PMID: 9683164.
7. Gabriel RS, Boisvert CJ, Mehta MC. Review of vitreopapillary traction syndrome. Neuroophthalmology. 2020;26;44(4):213–218. https://doi.org/10.1080/01658107.2020.1725063. PMID: 33012906; PMCID: PMC7518309.
8. Katz B, Hoyt WF. Gaze-evoked amaurosis from vitreopapillary traction. Am J Ophthalmol. 2005;139(4):631-7. https://doi.org/10.1016/j.ajo.2004.10.045. PMID: 15808158.
9. Cunha LP, Costa-Cunha LVF, Costa CF, Monteiro MLR. Ultrastructural changes detected using swept-source optical coherence tomography in severe vitreopapillary traction: a case report. Arq Bras Oftalmol. 2019;30;82(6):517–521. https://doi.org/10.5935/0004-2749.20190099. PMID: 31576923.
10. Romano MR, Vallejo-Garcia JL, Camesasca FI, Vinciguerra P, Costagliola C. Vitreo-papillary adhesion as a prognostic factor in pseudo- and lamellar macular holes. Eye (Lond). 2012;26(6):810-5. https://doi.org/10.1038/eye.2012.43. Epub 2012 Mar 16. PMID: 22422031; PMCID: PMC3376289.
11. Kesim C, Solmaz B, Pasaoglu I, Karslioglu MZ, Tatar I, Yildiz-Tas A, et al. Analysis of the peripapillary choroidal vascular characteristics in papilledema associated with pseudotumor cerebri. Optom Vis Sci. 2021;1;98(4):326–333.
12. Icoz M, Akdeniz M Peripapillary and subfoveal choroidal vascular index in patients with tension-type headache and migraine. Indian J Ophthalmol. 2024;72(5):S795-S800.
13. Sebag J. Classifying posterior vitreous detachment: a new way to look at the invisible. Br J Ophthalmol. 1997;81(7):521. https://doi.org/10.1136/bjo.81.7.521. PMID: 9290358; PMCID: PMC1722254.
14. Willekens K, Abegão Pinto L, Lemmens S, Bataillie S, Somers A, Vandewalle E, et al. The vitreopapillary interface in healthy and glaucoma: posterior vitreous detachment in the vitreopapillary interface study. Acta Ophthalmol. 2018;96(6):573–581. https://doi.org/10.1111/aos.13818. Epub 2018 Oct 2. PMID: 30280516.
15. Kim YH, Lee B, Kang E, Oh J. Peripapillary Choroidal Vascularity Outside the Macula in Patients With Central Serous Chorioretinopathy. Transl Vis Sci Technol. 2021;1;10(8):9. https://doi.org/10.1167/tvst.10.8.9. PMID: 34251422; PMCID: PMC8288056.
16. Parsa CF, Hoyt WF. Nonarteritic anterior ischemic optic neuropathy (NAION): a misnomer. Rearranging pieces of a puzzle to reveal a nonischemic papillopathy caused by vitreous separation. Ophthalmology. 2015;122(3):439 – 42. https://doi.org/10.1016/j.ophtha.2014.11.011. PMID: 25703466.
17. Li D, Sun S, Liang J, Yue Y, Yang J, Zhi Y, et al. Papillary vitreous detachment as a possible accomplice in non-arteritic anterior ischaemic optic neuropathy. Br J Ophthalmol. 2024;20;108(4):607–612.
18. Thompson AC, Bhatti MT, Gospe SM 3rd. Spectral-domain optical coherence tomography of the vitreopapillary interface in acute nonarteritic anterior ischemic optic neuropathy. Am J Ophthalmol. 2018 Nov;195:199–208. https://doi.org/10.1016/j.ajo.2018.08.002. Epub 2018 Aug 8. PMID: 30098345.
19. Katz B, Hoyt WF. Intrapapillary and peripapillary hemorrhage in young patients with incomplete posterior vitreous detachment. Signs of vitreopapillary traction. Ophthalmology. 1995;102(2):349 – 54. https://doi.org/10.1016/s0161-6420(95)31018-4. PMID: 7862424.
20. Nomura Y, Tamaki Y, Yanagi Y. Vitreopapillary traction diagnosed by spectral domain optical coherence tomography. Ophthalmic Surg Lasers Imaging. 2010;41:S74-6. https://doi.org/10.3928/15428877-20101031-16. PMID: 21117606.
21. Kim YW, Jeoung JW, Yu HG. Vitreopapillary traction in eyes with idiopathic epiretinal membrane: a spectral-domain optical coherence tomography study. Ophthalmology. 2014;121(10):1976-82. https://doi.org/10.1016/j.ophtha.2014.04.011. Epub 2014 May 29. PMID: 24880904.
22. Kroll P, Wiegand W, Schmidt J. Vitreopapillary traction in proliferative diabetic vitreoretinopathy [ssee comments]. Br J Ophthalmol. 1999;83(3):261-4. https://doi.org/10.1136/bjo.83.3.261. PMID: 10365029; PMCID: PMC1722969.

Publisher's note